axioms

Article

The Investigation of Dynamical Behavior of Benjamin–Bona–Mahony–Burger Equation with Different Differential Operators Using Two Analytical Approaches

Xiaoming Wang [1], Rimsha Ansar [2], Muhammad Abbas [2,*], Farah Aini Abdullah [3] and Khadijah M. Abualnaja [4]

1 School of Mathematics & Computer Science, Shangrao Normal University, Shangrao 334001, China
2 Department of Mathematics, University of Sargodha, Sargodha 40100, Pakistan
3 School of Mathematical Sciences, Universiti Sains Malaysia, Penang 11800, Malaysia
4 Department of Mathematics and Statistics, College of Science, Taif University, P.O. Box 11099, Taif 21944, Saudi Arabia
* Correspondence: muhammad.abbas@uos.edu.pk

Abstract: The dynamic behavior variation of the Benjamin–Bona–Mahony–Burger (BBM-Burger) equation has been investigated in this paper. The modified auxiliary equation method (MAEM) and Ricatti–Bernoulli (RB) sub-ODE method, two of the most reliable and useful analytical approaches, are used to construct soliton solutions for the proposed model. We demonstrate some of the extracted solutions using definitions of the β-derivative, conformable derivative (CD), and M-truncated derivatives (M-TD) to understand their dynamic behavior. The hyperbolic and trigonometric functions are used to derive the analytical solutions for the given model. As a consequence, dark, bell-shaped, anti-bell, M-shaped, W-shaped, kink soliton, and solitary wave soliton solutions are obtained. We observe the fractional parameter impact of the derivatives on physical phenomena. The BBM-Burger equation is functional in describing the propagation of long unidirectional waves in many nonlinear diffusive systems. The 2D and 3D graphs have been presented to confirm the behavior of analytical wave solutions.

Keywords: BBM-Burger equation; modified auxiliary equation method (MAEM); Ricatti–Bernoulli (RB) sub-ODE method; β-derivative; M-truncated derivative (M-TD); conformable derivative (CD); soliton solutions

MSC: 39A12; 39B62; 33B10; 26A48; 26A51

Citation: Wang, X.; Ansar, R.; Abbas, M.; Abdullah, F.A.; Abualnaja, K.M. The Investigation of Dynamical Behavior of Benjamin–Bona–Mahony–Burger Equation with Different Differential Operators Using Two Analytical Approaches. *Axioms* **2023**, *12*, 599. https://doi.org/10.3390/axioms12060599

Academic Editors: Hatıra Günerhan, Francisco Martínez González and Mohammed K. A. Kaabar

Received: 14 May 2023
Revised: 11 June 2023
Accepted: 14 June 2023
Published: 16 June 2023

1. Introduction

Nonlinear partial differential equations (NLPDEs) are frequently used in science and engineering to model a variety of nonlinear problems that can occur in real-life applications [1]. These equations, for instance, can be applied to the modeling of fluid dynamical issues, wave propagation in corrugated media, the study of earthquakes and seismic waves, and the modeling of optical fibers, among other things. The field of fluid dynamics is still important even if it is an older one that received a lot of attention. As an extension of differential equations (DEs) [2] of integer order, there are fractional order differential equations. Models of NLPDEs from physics and mathematics serve as essentials in theoretical sciences. Numerous practical fields, including meteorology, oceanography, and the aerospace industry, depend on a grasp of these NLPDEs.

Fractional differential equations (FDEs) [3] are becoming more and more prevalent today in a variety of disciplines, including dynamic systems and mathematics. Leibniz and L'Hôpital introduced the first idea for FDEs in 1695. In mathematical models incorporating FDEs, the nonlocal behavior of the fractional order derivatives provides the memory feature. Several researchers have been attracted to the flexibility of fractional theory and the numerous interesting features of fractional calculus (FC) [4–9]. New definitions of fractional derivatives were introduced by Caputo–Hadamard [10], Katugampola [11], Weyl [12], Riemann–Liouville [13], and Erdélyi–Kober [14], which enabled fractional calculus to deal with challenging natural phenomena. Throughout the past few decades, Caputo derivative [15] has been one of the most frequently employed fractional derivatives (FDs) in numerous research.

The mathematical model for small-amplitude long wave propagation in nonlinear dispersive media is described by the Benjamin–Bona–Mahony–Burger (BBM-Burger) equation [16]. The BBM equation has been proven to be preferable to the Korteweg–De Vries (KdV) [17] equation. The wave-breaking models are essential to the BBM-Burger equation and the KdV equation. The KdV equation was driven by water waves, and it was utilized in many other physical systems as a model for long waves. Solitary wave solutions of the BBM-Burger equation [18] reflect the dynamics of waves in the medium and are essential to many fields such as physics and dispersive systems [19]. In this study, the BBM-Burger equation is considered for analytical solutions in the sense of β-derivative, CD, and M-TD. In β-derivative, the proposed model has the following form

$$D^{\sigma}_{\beta,t}w - D^{\sigma}_{\beta,t}w_{zz} + w_z + \left(\frac{w^2}{2}\right)_z = 0, \tag{1}$$

where $D^{\sigma}_{\beta,t}$ is β-derivative and σ is fractional parameter.

In M-TD, the proposed model has the following form

$$D^{\sigma,\beta}_{j,t}w - D^{\sigma,\beta}_{j,t}w_{zz} + w_z + \left(\frac{w^2}{2}\right)_z = 0, \tag{2}$$

where $D^{\sigma,\beta}_{j,t}$ is M-TD and σ and β are fractional parameters.

In CD, the proposed model has the following form

$$D^{\sigma}_{c,t}w - D^{\sigma}_{c,t}w_{zz} + w_z + \left(\frac{w^2}{2}\right)_z = 0, \tag{3}$$

where $D^{\sigma}_{c,t}$ is CD and σ is fractional parameter.

The following is the BBM-Burger equation when β = 0 and σ = 1 are used.

$$w_t - w_{zzt} + w_z + \left(\frac{w^2}{2}\right)_z = 0. \tag{4}$$

Atangana was the one who first introduced the fractional "β-derivative" [20,21]. The recently introduced derivatives, which are used to depict various medical situations, meet a number of requirements that were previously thought to be limits for the fractional derivatives. Basic and satisfying most of the criteria for the classical integral derivative, the conformable fractional derivative definition includes linearity, Rolle's theorem, mean value theorem [22], product rule, quotient rule, power rule, and chain rule. The M-TD [23,24], which uses a Mittag–Leffler function with one parameter that satisfies several properties of integer-order calculus, was introduced in 2017 by Sousa and Oliveira. M-TD also satisfies the fundamental differential calculus mathematical principles, which stimulates additional research utilizing these newly formed notions. On conformable and M-TD models in the field of ocean engineering, there are some recent studies in the literature. The goal of these investigations is to find soliton solutions for the models with local derivatives. A novel solution for various FDEs is provided by the conformable fractional derivative, which aims to expand the ordinary derivative while satisfying some natural properties.

Numerous methods, including the extended $(\frac{G'}{G^2})$ expansion method [25], the multiple exp-function method [26], the M-lump solution [27], Sardar-subequation technique [28], the Jacobi elliptic function method (JEFM) [29], Painleve analysis, and many others, can be used to find the solitary wave solutions of NLPDEs. However, in this work, the MAEM and RB sub-ODE method [30] have been utilized for finding efficient and effective traveling wave solutions. The RB sub-ODE technique is originally created to produce precise traveling wave solutions, solitary wave solutions, and peaked wave solutions for NLPDEs. Backlund transformation is applied to the RB equation [31]. NLPDE [32,33] may be converted into a set of algebraic equations using the RB equation and a traveling wave transformation.

An approach for creating precise differential equation solutions is the MAEM [34]. The auxiliary equation approach has been expanded in this way. It offers a simple method for handling the solutions of nonlinear evolution equations. This effective method has been used to achieve findings that are pleasing and aid in the investigation of answers to numerous issues that are appearing in applied mathematics and physics. Although there are many different types of traveling wave solutions that may be built using exact solution techniques, approximation solution approaches are also useful when studying evolution equations. This study was inspired by recent developments in fractional nonlinear evolution equations' traveling wave solutions. Recently, it has been discovered that a variety of exact solution techniques are useful in creating potential wave behaviors that correspond to the physical system defined by a specific evolution equation. Reading the published research papers [21,24,35–38] also inspired the authors. In this paper, we use two effective analytical approaches to derive the precise soliton solutions of the BBM-Burger equation while taking into account three natural extensions of the classical derivative, namely the *beta*-derivative, M-TD, and CD. Additionally, using the Wolfram Mathematica 12 software, we provide several 2D and 3D graphical representations of the analytical soliton solutions of the BBM-Burger equation and investigate the impact of the fractional parameters employed in *beta*-derivative, M-TD, and CD.

This paper is organized as follows: Basic definitions and their properties are explained in Section 2. Section 3 represents the mathematical interpretation of the BBM-Burger equation. Sections 4 and 5 conduct the algorithmic steps of the RB-sub ODE method and MAEM and apply them to the proposed model. In addition to computing, graphs are used to show how the result can be physically explained in Section 6. In Section 7, there are some concluding remarks to wrap up the work.

2. Preliminaries

The definitions of derivatives along with their fundamental properties are discussed in this section.

2.1. β-Derivative and Its Properties

Definition 1. *The β-derivative is another kind of conformable derivative that can be defined, as [20]*

$$D^{\sigma}_{\beta,t}w(t) = \lim_{\varepsilon\to 0}\frac{w(t+\varepsilon(t+\frac{1}{\Gamma(\sigma)})^{1-\sigma}) - w(t)}{\varepsilon}, \quad 0<\sigma\leq 1.$$

The β-derivative has the following properties.

- The β-derivative is a linear operator; $D^{\sigma}_{\beta,t}(cd(z)+rq(z)) = c\,D^{\sigma}_{\beta,t}d(z) + rD^{\sigma}_{\beta,t}q(z)$, $\forall c, r \in \Re$.
- It satisfies the product rule; $D^{\sigma}_{\beta,t}(d(z)*q(z)) = q(z)D^{\sigma}_{\beta,t}d(z) + d(z)D^{\sigma}_{\beta,t}q(z)$.
- It satisfies the quotient rule; $D^{\sigma}_{\beta,t}\left\{\frac{d(z)}{q(z)}\right\} = \frac{q(z)D^{\sigma}_{\beta,t}d(z) - d(z)D^{\sigma}_{\beta,t}q(z)}{q^2(z)}$.
- The β-derivative of a constant is zero; $D^{\sigma}_{\beta,t}(c) = 0$, for any constant c.

2.2. M-Truncated Derivative and Its Properties

This section defines an M-TD and presents several results that are surprisingly similar to those of classical calculus. Sousa et al. [39] recently presented the M-TD, which is a natural extension of the ordinary derivative. This derivative does not have the shortcomings of the preceding ones. The M-TD is also known as a conformable fractional derivative [23,40].

The M-TD can readily satisfy some features of classical calculus, including the quotient rule, product rule, linearity, chain rule, and function composition rule. The M-TD, which makes use of a one-parameter Mittag–Leffler function, also satisfies the requirements of integer-order calculus.

Definition 2. *The M-TD for the function $w : [0, \infty) \to R$ of order $\sigma \in (0, 1)$ is defined, as [35]*

$$D^{\sigma,\beta}_{j,t} w(t) = \frac{\lim_{\varepsilon\to 0} w(tE^{\beta}_{j}(\varepsilon t^{-\sigma})) - w(t),}{\varepsilon}$$

for $t > 0$. Where $E^{\beta}_{j}(.), \beta > 0$ is a truncated Mittag–Leffler function of one parameter defined, as:

$$E^{\beta}_{j}(t) = \sum_{k=0}^{j} \frac{t^k}{\Gamma(\beta k + 1)}.$$

The M-TD has the following properties.

- The M-TD is a linear operator; $D^{\sigma,\beta}_{j,z}(cd(z) + rq(z)) = cD^{\sigma,\beta}_{j,z} d(z) + rD^{\sigma,\beta}_{j,z} q(z)$, $\forall\, c, r \in \Re$.
- It satisfies the product rule; $D^{\sigma,\beta}_{j,z}(d(z) * q(z)) = q(z)D^{\sigma,\beta}_{j,z} d(z) + d(z)D^{\sigma,\beta}_{j,z} q(z)$.
- It satisfies the quotient rule; $D^{\sigma,\beta}_{j,z}\left\{\frac{d(z)}{q(z)}\right\} = \frac{q(z)D^{\sigma,\beta}_{j,z} d(z) - d(z)D^{\sigma,\beta}_{j,z} q(z)}{q^2(z)}$.
- The M-TD for a differentiable function $q(z)$ is defined, as:

$$D^{\sigma,\beta}_{j,z} q(z) = \frac{z^{1-\sigma}}{\Gamma(\beta+1)} \frac{dq}{dz}.$$

2.3. Conformable Derivative

Definition 3. *The conformable derivative of order σ for a function $w : [0, \infty) \to \Re$ is written as:*

$$D^{\sigma}_{c,t} w(t) = \lim_{\varepsilon\to 0} \frac{w(t + \varepsilon(t)^{1-\sigma}) - w(t)}{\varepsilon}, \quad \forall t > 0.$$

If w has σ-differentiability in any interval $(0, a)$ with $a > 0$, then

$$D^{\sigma}_{c}(w(0)) = \lim_{t\to 0^+} D^{\sigma}_{c}(w(t)),$$

whenever the limit of the right-hand side exists.

Further, properties and theorems related to CD are discussed in [37].

3. Mathematical Interpretation of the Proposed Model

To obtain soliton solutions for Equation (4), the following transformations have been employed.

$$W(z, t) = w(\eta). \tag{5}$$

Three definitions are provided for the traveling wave parameter η.

For β-derivative, η has the following form

$$\eta = Kz + \frac{R}{\sigma}\left(t + \frac{1}{\Gamma(\sigma)}\right)^{\sigma}. \tag{6}$$

For M-TD, η has the following form

$$\eta = Kz + \frac{R\Gamma(\beta+1)}{\sigma} t^{\sigma}. \tag{7}$$

For CD, η has the following form

$$\eta = Kz + \frac{R}{\sigma} t^{\sigma}, \tag{8}$$

where K, R are arbitrary constants with $K, R \neq 0$. Utilizing the transformation Equation (5) together with Equations (6)–(8), the obtained ordinary differential equation is

$$(K + R)w' - K^2 R w''' + w w' K = 0.$$

This, when integrated with the integration constant set to zero, yields

$$(K + R)w - K^2 R w'' + \frac{w^2}{2} K = 0, \tag{9}$$

where $w' = \frac{dw}{d\eta}$.

4. Application of RB Sub-ODE Method

According to RB sub-ODE method [30], the solution for Equation (9) is

$$w' = H_1 w^{2-L} + F_1 w + G_1 w^L, \tag{10}$$

where the constants H_1, F_1, G_1, and L will be found later.

Substituting Equation (10) into Equation (9), we have

$$\begin{aligned} -3K^2 R F_1 H_1 w(\eta)^2 + K^2 L R F_1 H_1 w(\eta)^2 - 2K^2 R H_1^2 w(\eta)^{3-L} + K^2 L R H_1^2 w(\eta)^{3-L} \\ -K^2 R F_1 G_1 w(\eta)^{2L} - K^2 L R F_1 G_1 w(\eta)^{2L} + K w(\eta)^{1+L} + R w(\eta)^{1+L} - K^2 R F_1^2 w(\eta)^{1+L} \\ -2K^2 R G_1 H_1 w(\eta)^{1+L} + \frac{1}{2} K w(\eta)^{2+L} - K^2 L R G_1^2 w(\eta)^{-1+3L} = 0. \end{aligned} \tag{11}$$

Setting $L = 0$ in the above equation, we obtain

$$\begin{aligned} -K^2 R F_1 G_1 + K w(\eta) + R w(\eta) - K^2 R F_1^2 w(\eta) - 2K^2 R G_1 H_1 w(\eta) + \frac{1}{2} K w(\eta)^2 \\ -3K^2 R F_1 H_1 w(\eta)^2 - 2K^2 R H_1^2 w(\eta)^3. \end{aligned} \tag{12}$$

Adjusting each coefficient of $w^i (i = 0, 1, 2, 3)$ to zero, we have

$$\begin{aligned} -K^2 R F_1 G_1 &= 0, \\ K + R - K^2 R F_1^2 - 2K^2 R G_1 H_1 &= 0, \\ \frac{K}{2} - 3K^2 R F_1 H_1 &= 0, \\ -2K^2 R H_1^2 &= 0. \end{aligned} \tag{13}$$

Equation (13) produces the following results when it is solved.

$$H_1 = \mp \frac{1}{6\sqrt{R}\sqrt{K + R}}, F_1 = \mp \frac{\sqrt{K + R}}{K\sqrt{R}}, G_1 = 0.$$

Case 1.
when $L \neq 1, F_1 \neq 0$ and $G_1 = 0$, the algebraic solution can be obtained.

$$w(\eta) = \left(-\frac{H_1}{F_1} + P e^{F_1 (L-1)\eta} \right)^{\frac{1}{L-1}}, \tag{14}$$

$$W_{1,1}(z,t) = \frac{1}{\left(e^{\frac{3\sqrt{K+R}\eta}{K\sqrt{R}}}P - \frac{K}{6(K+R)}\right)^{1/3}}.$$

Case 2.
when $L \neq 1, H_1 \neq 0$ and $F_1{}^2 - 4H_1G_1 < 0$, the solitary periodic solutions can be obtained.

$$w(\eta) = \left(-\frac{F_1}{2H_1} + \frac{\sqrt{4H_1G_1 - (F_1)^2}}{2H_1}\tan\left(\frac{(1-L)\sqrt{4H_1G_1 - (F_1)^2}}{2}(\eta + P)\right)\right)^{\frac{1}{1-L}}, \tag{15}$$

$$W_{1,2}(z,t) = \left(-\frac{3(K+R)}{K} - 3\sqrt{R}\sqrt{K+R}\sqrt{-\frac{K+R}{K^2R}}\tan\left(\frac{3}{2}\sqrt{-\frac{K+R}{K^2R}}(P+\eta)\right)\right)^{1/3}.$$

and

$$w(\eta) = \left(-\frac{F_1}{2H_1} - \frac{\sqrt{4H_1G_1 - (F_1)^2}}{2H_1}\cot\left(\frac{(1-L)\sqrt{4H_1G_1 - (F_1)^2}}{2}(\eta + P)\right)\right)^{\frac{1}{1-L}}, \tag{16}$$

$$W_{1,3}(z,t) = \left(-\frac{3(K+R)}{K} - 3\sqrt{R}\sqrt{K+R}\sqrt{-\frac{K+R}{K^2R}}\cot\left(\frac{3}{2}\sqrt{-\frac{K+R}{K^2R}}(P+\eta)\right)\right)^{1/3}.$$

Case 3.
when $L \neq 1, H_1 \neq 0$ and $F_1{}^2 - 4H_1G_1 > 0$, these dark optical and solitary optical soliton solutions are found, respectively.

$$w(\eta) = \left(-\frac{F_1}{2H_1} - \frac{\sqrt{-4H_1G_1 + (F_1)^2}}{2H_1}\coth\left(\frac{(1-L)\sqrt{-4H_1G_1 + (F_1)^2}}{2}(\eta + P)\right)\right)^{\frac{1}{1-L}}, \tag{17}$$

$$W_{1,4}(z,t) = \left(-\frac{3(K+R)}{K} - 3\sqrt{R}\sqrt{K+R}\sqrt{\frac{K+R}{K^2R}}\coth\left(\frac{3}{2}\sqrt{\frac{K+R}{K^2R}}(P+\eta)\right)\right)^{1/3}.$$

and

$$w(\eta) = \left(-\frac{F_1}{2H_1} + \frac{\sqrt{-4H_1G_1 + (F_1)^2}}{2H_1}\tanh\left(\frac{(1-L)\sqrt{-4H_1G_1 + (F_1)^2}}{2}(\eta + P)\right)\right)^{\frac{1}{1-L}}, \tag{18}$$

$$W_{1,5}(z,t) = \left(-\frac{3(K+R)}{K} - 3\sqrt{R}\sqrt{K+R}\sqrt{\frac{K+R}{K^2R}}\tanh\left(\frac{3}{2}\sqrt{\frac{K+R}{K^2R}}(P+\eta)\right)\right)^{1/3}.$$

Case 4.
when $L \neq 1, H_1 \neq 0$ and $F_1{}^2 - 4H_1G_1 = 0$, the following algebraic solution is found.

$$w(\eta) = \left(-\frac{F_1}{2H_1} + \frac{1}{H_1(L-1)(\eta + P)}\right)^{\frac{1}{1-L}}, \tag{19}$$

$$W_{1,6}(z,t) = \left(-\frac{3(K+R)}{K} + \frac{2\sqrt{R}\sqrt{K+R}}{P+\eta}\right)^{1/3}.$$

Case 5.
when $L \neq 1, H_1 \neq 0$ and $G_1 = 0$, the following solution is obtained.

$$w(\eta) = (H_1(L-1)(\eta+P))^{\frac{1}{L-1}}, \tag{20}$$

$$W_{1,7}(z,t) = \frac{\left(\frac{3}{2}\right)^{1/4}}{\left(\frac{P+\eta}{\sqrt{R}\sqrt{K+R}}\right)^{1/4}}.$$

where P is an arbitrary constant.

5. Utilizing the MAEM

For obtaining the solutions, the MAEM [34] provides the general solution in the form

$$w(\eta) = H_0 + \sum_{k=1}^{m}\left[H_K(\phi^h)^k + F_k(\phi^h)^{-k}\right], \tag{21}$$

where H_0, H_k's and F_k's are unknown constants. The auxiliary equation defines the function $h(\eta)$.

$$h'(\eta) = \frac{s + m\phi^{-h} + n\phi^h}{\ln \phi}, \tag{22}$$

for arbitrary constant values of s, m and n $(\phi > 0, \phi \neq 1)$.

Cases for the Equation (22) are discussed below.

1. If $s^2 - 4mn < 0$ and $n \neq 0$, then, $\phi^{h(\eta)} = \frac{-s+\sqrt{4mn-s^2}\tan\left(\frac{\sqrt{4mn-s^2}\eta}{2}\right)}{2n}$, or $\phi^{h(\eta)} = -\frac{s+\sqrt{4mn-s^2}cot\left(\frac{\sqrt{4mn-s^2}\eta}{2}\right)}{2n}$.
2. If $s^2 - 4mn > 0$ and $n \neq 0$, then, $\phi^{h(\eta)} = -\frac{s+\sqrt{s^2-4mn}\tanh\left(\frac{\sqrt{s^2-4mn}\eta}{2}\right)}{2n}$, or $\phi^{h(\eta)} = -\frac{s+\sqrt{s^2-4mn}\coth\left(\frac{\sqrt{s^2-4mn}\eta}{2}\right)}{2n}$.
3. If $s^2 - 4mn = 0$ and $n \neq 0$, then, $\phi^{h(\eta)} = -\frac{2+s\eta}{2n\eta}$.

The highest order derivative w'' and the highest order nonlinear term w^2 in Equation (9) are balanced according to the homogeneous balance principle, yields that $m = 2$, gives

$$w(\eta) = H_0 + H_1\phi^h + F_1\phi^{-h} + H_2\phi^{2h} + F_2\phi^{-2h}. \tag{23}$$

The following set of algebraic equations is obtained by equating each coefficient of $\phi^{h(\eta)}$ to zero:

$$\phi^{h(\eta)^{-4}} : \tfrac{1}{2}KF_2\left(-12Km^2R + F_2\right) = 0,$$
$$\phi^{h(\eta)^{-3}} : K\left(-10KmRsF_2 + F_1\left(-2Km^2R + F_2\right)\right) = 0,$$
$$\phi^{h(\eta)^{-2}} : -3K^2mRsF_1 + \frac{KF_1^2}{2} + F_2\left(K + R - 4K^2R\left(2mn + s^2\right) + KH_0\right) = 0,$$
$$\phi^{h(\eta)^{-1}} : F_1\left(K + R - K^2R\left(2mn + s^2\right) + KH_0\right) + KF_2\left(-6KnRs + H_1\right) = 0,$$
$$\phi^{h(\eta)^{0}} : -K^2nRsF_1 - 2K^2n^2RF_2 + KH_0 + RH_0 + \frac{KH_0^2}{2} - K^2mRsH_1 + KF_1H_1 - 2K^2m^2RH_2 + KF_2H_2 = 0,$$
$$\phi^{h(\eta)^{1}} : \left(K + R - K^2R\left(2mn + s^2\right) + KH_0\right)H_1 + K(-6KmRs + F_1)H_2 = 0,$$
$$\phi^{h(\eta)^{2}} : -3K^2nRsH_1 + \frac{KH_1^2}{2} + \left(K + R - 4K^2R\left(2mn + s^2\right) + KH_0\right)H_2 = 0,$$
$$\phi^{h(\eta)^{3}} : K\left(-10KnRsH_2 + H_1\left(-2Kn^2R + H_2\right)\right) = 0,$$
$$\phi^{h(\eta)^{4}} : K\left(-10KnRsH_2 + H_1\left(-2Kn^2R + H_2\right)\right) = 0.$$

Solving the above equations, yields, the following families.

Family 1:

when $H_0 = \frac{-K-R+8K^2mnR+K^2Rs^2}{K}, H_1 = 12KnRs, H_2 = 12Kn^2R, F_1 = 0, F_2 = 0.$
The following cases have occurred.

- For $s^2 - 4mn < 0$ and $n \neq 0$, the trigonometric solutions are found.

$$W_{1,1}(z,t) = -1 - \frac{R}{K} + 8KmnR - 2KRs^2 + 3KR\left(4mn - s^2\right) \tan\left(\frac{1}{2}\sqrt{4mn - s^2}\eta\right)^2,$$

or

$$W_{1,2}(z,t) = -1 - \frac{R}{K} + KR\left(4mn - s^2\right)\left(-1 + 3\csc\left(\frac{1}{2}\sqrt{4mn - s^2}\eta\right)^2\right).$$

- For $s^2 - 4mn > 0$ and $n \neq 0$, the hyperbolic solutions are obtained.

$$W_{1,3}(z,t) = -1 - \frac{R}{K} + 8KmnR - 2KRs^2 + 3KR\left(-4mn + s^2\right) \tanh\left(\frac{1}{2}\sqrt{-4mn + s^2}\eta\right)^2,$$

or

$$W_{1,4}(z,t) = -1 - \frac{R}{K} + 8KmnR - 2KRs^2 + 3KR\left(-4mn + s^2\right) \coth\left(\frac{1}{2}\sqrt{-4mn + s^2}\eta\right)^2.$$

Family 2:

When $H_0 = \frac{-K-R+8K^2mnR+K^2Rs^2}{K}, H_1 = 0, H_2 = 0, F_1 = 12KmRs, F_2 = 12Km^2R.$
The following cases are obtained.

- For $s^2 - 4mn < 0$ and $n \neq 0$, the following trigonometric solutions resulted.

$$W_{2,1}(z,t) = -1 - \frac{R}{K} + KR\left(s^2 + 8mn\left(1 + \frac{3\left(2mn - s^2 + s\sqrt{4mn - s^2}\tan\left(\frac{1}{2}\sqrt{4mn - s^2}\eta\right)\right)}{\left(s - \sqrt{4mn - s^2}\tan\left(\frac{1}{2}\sqrt{4mn - s^2}\eta\right)\right)^2}\right)\right),$$

or

$$W_{2,2}(z,t) = -1 - \frac{R}{K} + KR\left(s^2 + 8mn\left(\begin{array}{c} 1 + \frac{6mn}{\left(s+\sqrt{4mn-s^2}\cot\left(\frac{1}{2}\sqrt{4mn-s^2}\eta\right)\right)^2} \\ -\frac{3s}{s+\sqrt{4mn-s^2}\cot\left(\frac{1}{2}\sqrt{4mn-s^2}\eta\right)} \end{array}\right)\right).$$

- For $s^2 - 4mn > 0$ and $n \neq 0$, the following hyperbolic solutions are found.

$$W_{2,3}(z,t) = -1 - \frac{R}{K} + KR\left(s^2 + 8mn\left(\begin{array}{c} 1 + \frac{6mn}{\left(s+\sqrt{-4mn+s^2}\tanh\left(\frac{1}{2}\sqrt{-4mn+s^2}\eta\right)\right)^2} \\ -\frac{3s}{s+\sqrt{-4mn+s^2}\tanh\left(\frac{1}{2}\sqrt{-4mn+s^2}\eta\right)} \end{array}\right)\right),$$

or

$$W_{2,4}(z,t) = -1 - \frac{R}{K} + KR\left(s^2 + 8mn\left(\begin{array}{c} 1 + \frac{6mn}{\left(s+\sqrt{-4mn+s^2}\coth\left(\frac{1}{2}\sqrt{-4mn+s^2}\eta\right)\right)^2} \\ -\frac{3s}{s+\sqrt{-4mn+s^2}\coth\left(\frac{1}{2}\sqrt{-4mn+s^2}\eta\right)} \end{array}\right)\right).$$

Family 3:

When $H_0 = \frac{-K-R+8K^2mnR+K^2Rs^2}{K}, H_1 = 12KnRs, H_2 = 12Kn^2R, F_1 = 12KmRs, F_2 = 12Km^2R.$

The cases listed below have occurred.

- For $s^2 - 4mn < 0$ and $n \neq 0$, the trigonometric solutions are found.

$$W_{3,1}(z,t) = -1 - \frac{R}{K} - 2KRs^2 + 3KR\left(4mn - s^2\right)\tan\left(\frac{1}{2}\sqrt{4mn - s^2}\eta\right)^2 + 8KmnR\left(1 + \frac{3\left(2mn - s^2 + s\sqrt{4mn - s^2}\tan\left(\frac{1}{2}\sqrt{4mn - s^2}\eta\right)\right)}{\left(s - \sqrt{4mn - s^2}\tan\left(\frac{1}{2}\sqrt{4mn - s^2}\eta\right)\right)^2}\right),$$

or

$$W_{3,2}(z,t) = -1 - \frac{R}{K} - 2KRs^2 + 3KR\left(4mn - s^2\right)\cot\left(\frac{1}{2}\sqrt{4mn - s^2}\eta\right)^2 + 8KmnR\left(\begin{array}{c} 1 + \frac{6mn}{\left(s + \sqrt{4mn - s^2}\cot\left(\frac{1}{2}\sqrt{4mn - s^2}\eta\right)\right)^2} \\ - \frac{3s}{s + \sqrt{4mn - s^2}\cot\left(\frac{1}{2}\sqrt{4mn - s^2}\eta\right)} \end{array}\right).$$

- For $s^2 - 4mn > 0$ and $n \neq 0$, the following hyperbolic solutions are obtained.

$$W_{3,3}(z,t) = -1 - \frac{R}{K} - 2KRs^2 + 3KR\left(-4mn + s^2\right)\tanh\left(\frac{1}{2}\sqrt{-4mn + s^2}\eta\right)^2 + 8KmnR\left(\begin{array}{c} 1 + \frac{6mn}{\left(s + \sqrt{-4mn + s^2}\tanh\left(\frac{1}{2}\sqrt{-4mn + s^2}\eta\right)\right)^2} \\ - \frac{3s}{s + \sqrt{-4mn + s^2}\tanh\left(\frac{1}{2}\sqrt{-4mn + s^2}\eta\right)} \end{array}\right),$$

or

$$W_{3,4}(z,t) = -1 - \frac{R}{K} - 2KRs^2 + 3KR\left(-4mn + s^2\right)\coth\left(\frac{1}{2}\sqrt{-4mn + s^2}\eta\right)^2 + 8KmnR\left(\begin{array}{c} 1 + \frac{6mn}{\left(s + \sqrt{-4mn + s^2}\coth\left(\frac{1}{2}\sqrt{-4mn + s^2}\eta\right)\right)^2} \\ - \frac{3s}{s + \sqrt{-4mn + s^2}\coth\left(\frac{1}{2}\sqrt{-4mn + s^2}\eta\right)} \end{array}\right).$$

6. Graphical Illustration

This section provides a graphical representation of the BBM-Burger equation solutions that have been found. Concerning the 2D and 3D graphs of $W_{1,1}(z,t)$, $W_{1,3}(z,t)$, $W_{1,4}(z,t)$, respectively, provided the periodic and single wave solutions for the values $\sigma = 0.5, 1$, $\mathrm{P} = 1.7, 5.5$, $\mathrm{K} = 14.5, 15.5$, $\mathrm{R} = -0.5$, $\beta = 0.35$, within the interval $-5 \leq z \leq 5, 0 \leq t \leq 2$ for 3D graph and $\mathrm{t} = 1$ for 2D plots, as shown in Figures 1–3 by RB sub-ODE method. Figures 4 and 5 represent the Kink and Pulse shape soliton 3D solutions of $W_{1,5}(z,t)$ and $W_{1,6}(z,t)$ for the values $\sigma = 0.5$, $\mathrm{P} = -1.7, 5.5$, $\mathrm{K} = 14.5, 10.5$, $\mathrm{R} = 14.5, 0.5$, $\beta = 0.35$ and 2D plots at $\mathrm{t} = 1$ for the same values in the interval $-5 \leq z \leq 5, 0 \leq t \leq 2$ by RB sub-ODE method.

The solutions for the trigonometric and hyperbolic functions in $W_{1,1}(z,t)$ and $W_{1,3}(z,t)$ are that we obtain the anti-bell-shaped solitons and dark soliton solutions, respectively, by choosing the values $\sigma = 0.5$, $\mathrm{m} = 1$, $\mathrm{K} = 2$, $\mathrm{R} = 1$, $\beta = 0.35$, $\mathrm{s} = 0.1$, $\mathrm{n} = 1$, within the range $-10 \leq z \leq 10, -10 \leq t \leq 10$, and $\mathrm{t} = 1$ for 2D surfaces in Figures 6 and 7 by MAEM. The dark soliton solution, in which the intensity profile of the soliton displays a dip in a uniform backdrop, this hole-soliton, often referred to as a dark soliton, causes a transient reduction in wave amplitude. Solutions for the Family 2 in $W_{2,1}(z,t)$ and $W_{2,3}(z,t)$, by MAEM provides the bright and bell-shaped soliton solutions by taking the values $\sigma = 0.5$, $\mathrm{m} = 1$, $\mathrm{K} = -2.5$, $\mathrm{R} = 1$, $\beta = 0.35$, $\mathrm{s} = 0.1$, $\mathrm{n} = 1$, within the range $-10 \leq z \leq 10, -10 \leq t \leq 10$, and $\mathrm{t} = 1$ for 2D surfaces in Figures 8 and 9.

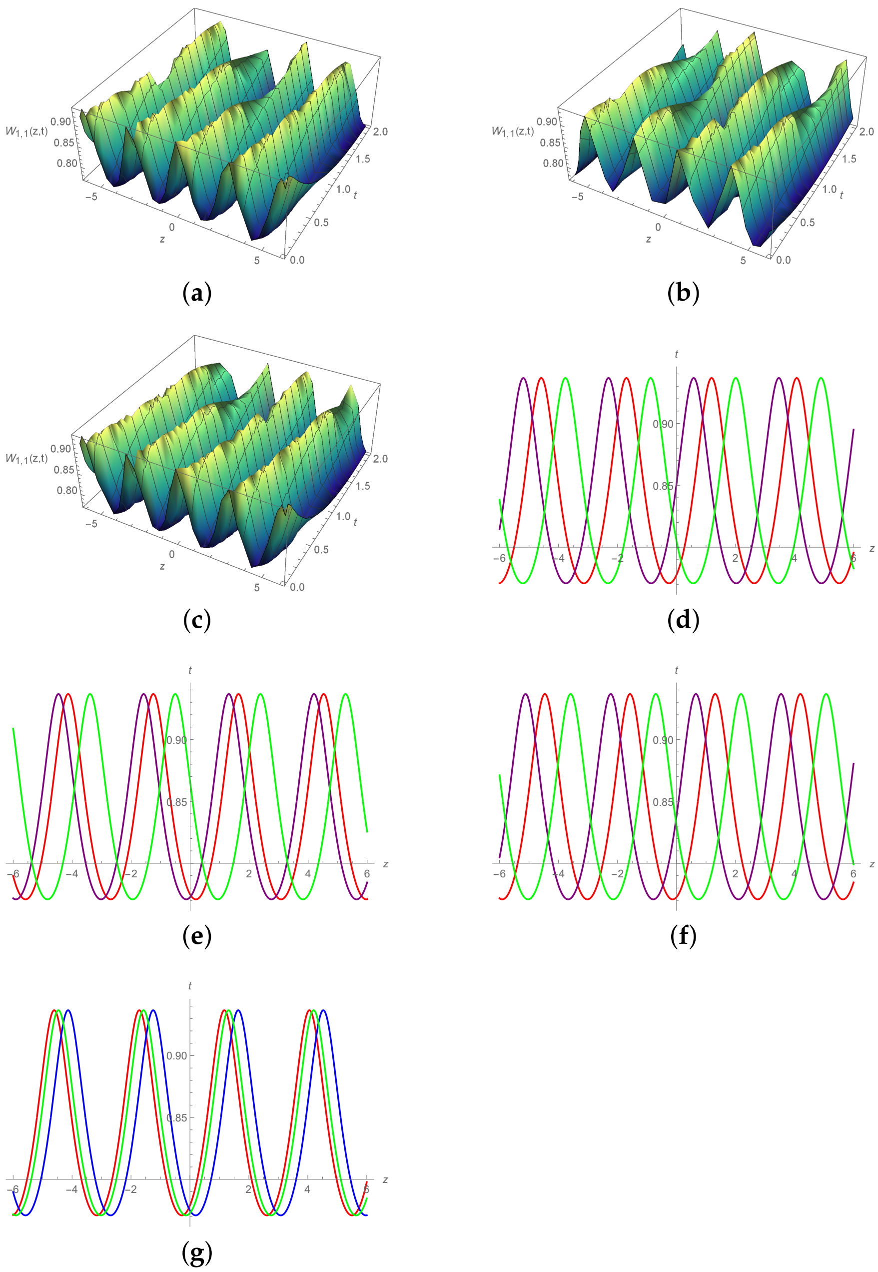

Figure 1. Graphical representation of analytical solution $W_{1,1}(z,t)$ by RB sub-ODE method, when $\sigma = 0.5, P = 1.7, K = 14.5, R = -9.5, \beta = 0.35$. (**a**) M-TD 3D graph at $\sigma = 0.5$; (**b**) β-derivative 3D graph at $\sigma = 0.5$; (**c**) CD 3D graph at $\sigma = 0.5$; (**d**) 2D plot of M-TD at different values of $\sigma = 0.5$, $\beta = 0.25$ (red), $\sigma = 1$, $\beta = 0.5$ (purple), $\sigma = 0.3$, $\beta = 0.75$ (green); (**e**) 2D plot of β-derivative at different values of $\sigma = 0.5$ (red), 1 (purple), 0.3 (green); (**f**) 2D plot of CD at different values of $\sigma = 0.5$ (red), 1 (purple), 0.3 (green); (**g**) A comparison between M-TD (red), β-derivative (blue) and CD (green) at $\sigma = 0.5$. (**d**–**g**) 2D comparison plots at $t = 1$.

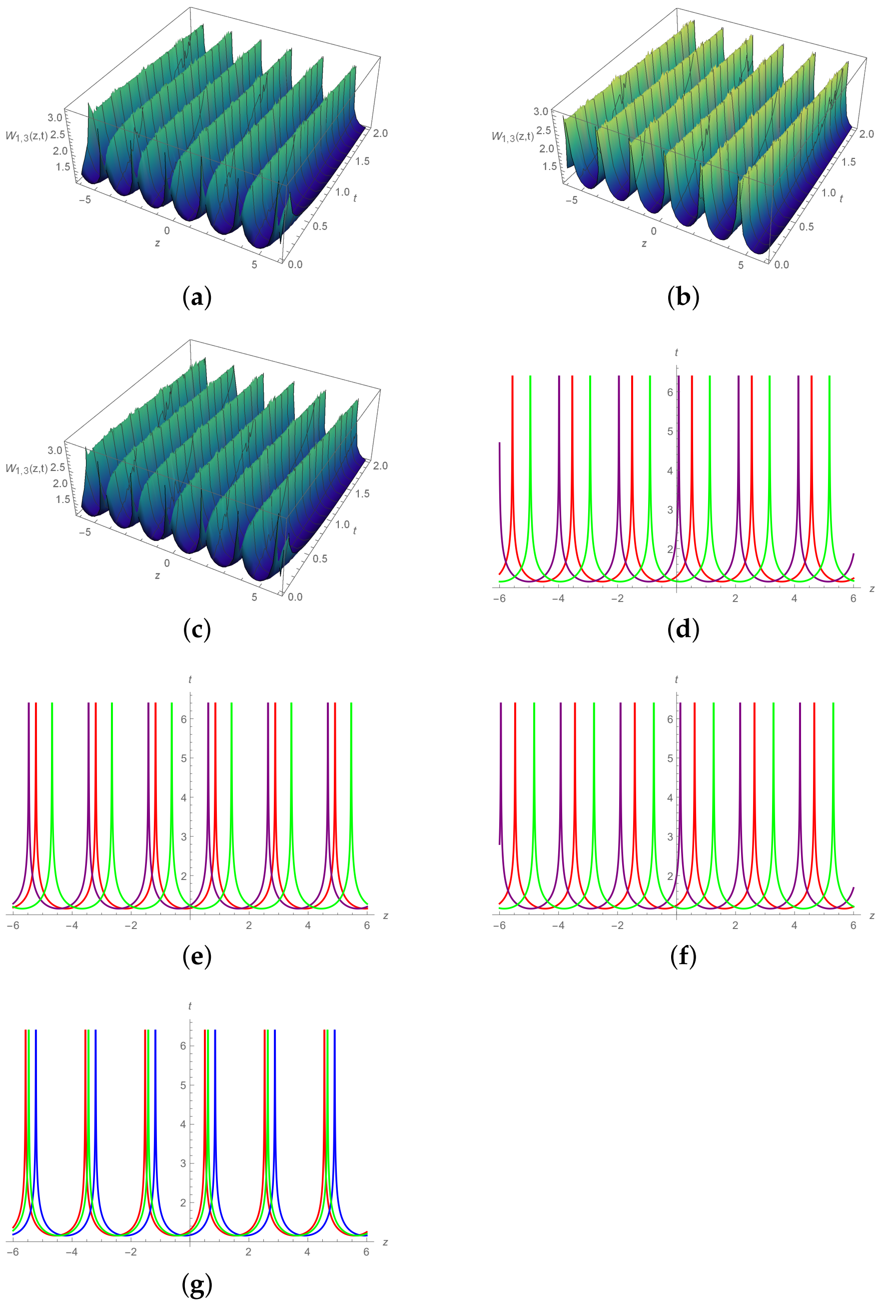

Figure 2. Graphical representation of analytical solution $W_{1,3}(z,t)$ by RB sub-ODE method, when $\sigma = 0.5, P = 5.5, K = 15.5, R = -7.5, \beta = 0.35$. (**a**) M-TD 3D graph at σ = 0.5; (**b**) β-derivative 3D graph at σ = 0.5; (**c**) CD 3D graph at σ = 0.5; (**d**) 2D plot of M-TD at different values of σ = 0.5, β = 0.25 (red), σ = 1, β =0.5 (purple), σ = 0.3, β =0.75 (green); (**e**) 2D plot of β-derivative at different values of σ = 0.5 (red), 1 (purple), 0.3 (green); (**f**) 2D plot of CD at different values of σ = 0.5 (red), 1 (purple), 0.3 (green); (**g**) A comparison between M-TD (red), β-derivative (blue) and CD (green) at $\sigma = 0.5$. (**d**–**g**) 2D comparison plots at $t = 1$.

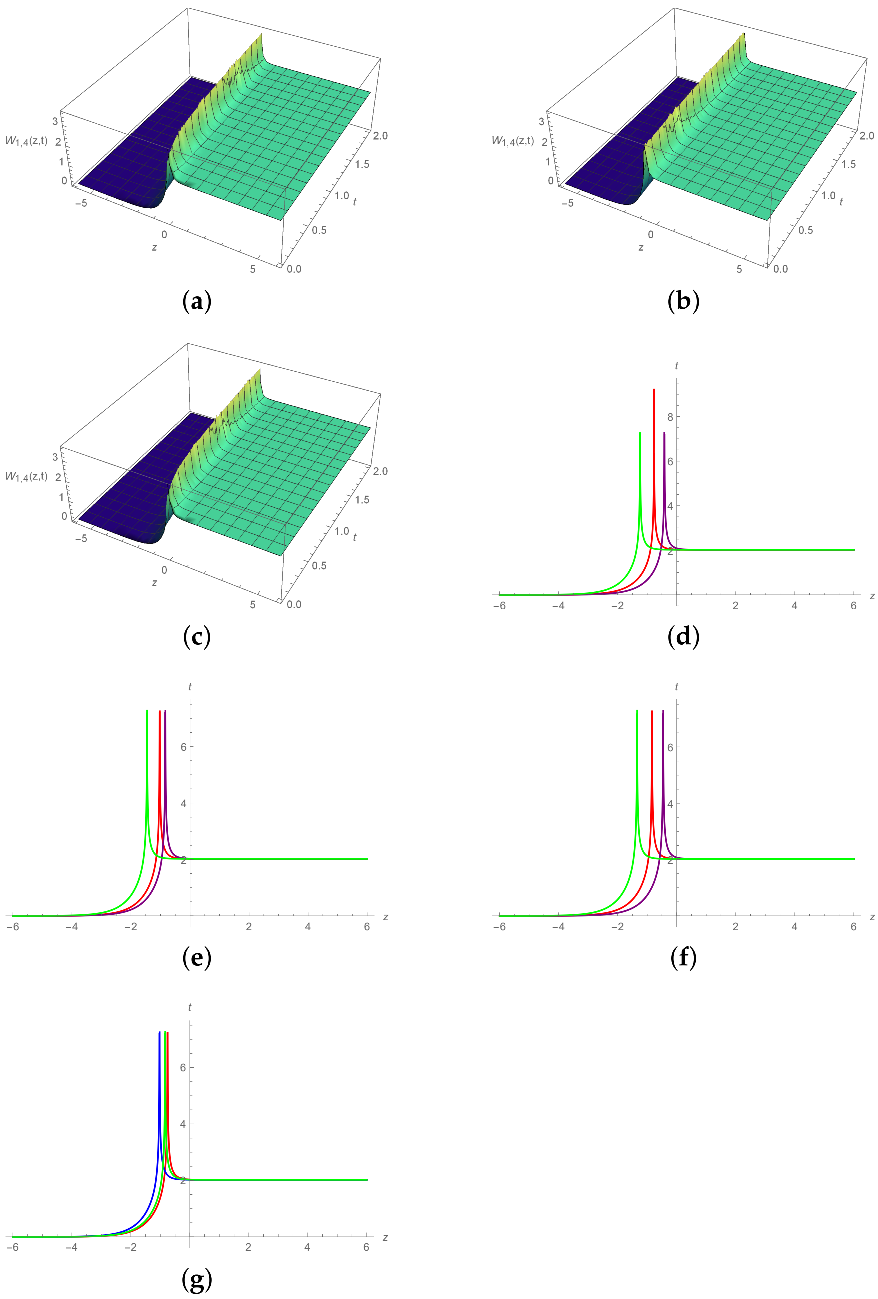

Figure 3. Graphical representation of analytical solution $W_{1,4}(z,t)$ by RB sub-ODE method, when $\sigma = 0.5, P = 1.5, K = 18.5, R = 7, \beta = 0.35$. (**a**) M-TD 3D graph at σ = 0.5; (**b**) β-derivative 3D graph at σ = 0.5; (**c**) CD 3D graph at σ = 0.5; (**d**) 2D plot of M-TD at different values of σ = 0.5, β = 0.25 (red), σ = 1, β = 0.5 (purple), σ = 0.3, β = 0.75 (green); (**e**) 2D plot of β-derivative at different values of σ = 0.5 (red), 1 (purple), 0.3 (green); (**f**) 2D plot of CD at different values of σ = 0.5 (red), 1 (purple), 0.3 (green); (**g**) A comparison between M-TD (red), β-derivative (blue) and CD (green) at $\sigma = 0.5$. (**d**–**g**) 2D comparison plots at $t = 1$.

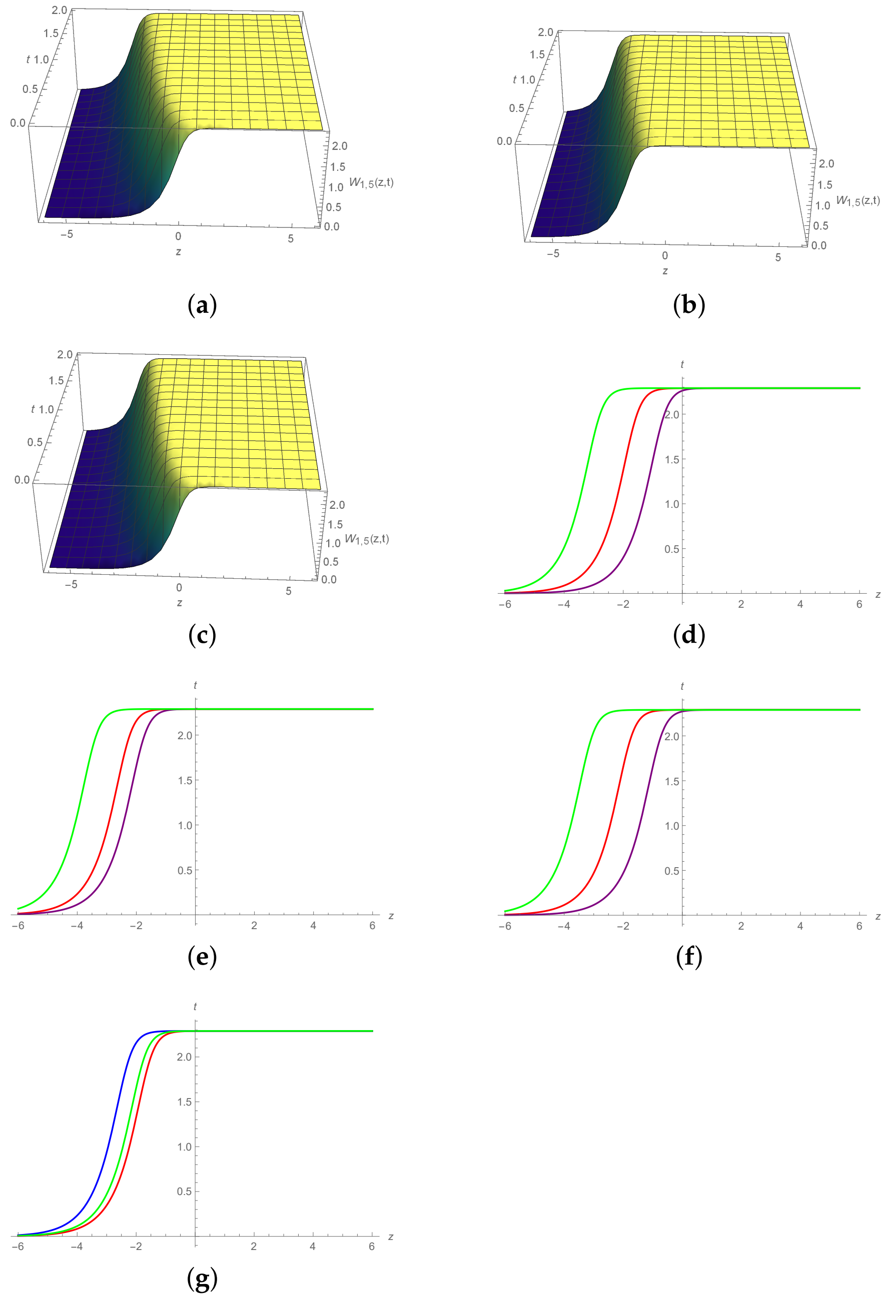

Figure 4. Graphical representation of analytical solution $W_{1,5}(z,t)$ by RB sub-ODE method, when $\sigma = 0.5, P = -1.7, K = 14.5, R = 14.5, \beta = 0.35$. (**a**) M-TD 3D graph at σ = 0.5; (**b**) β-derivative 3D graph at σ = 0.5; (**c**) CD 3D graph at σ = 0.5; (**d**) 2D plot of M-TD at different values of σ = 0.5, β = 0.25 (red), σ = 1, β = 0.5 (purple), σ = 0.3, β = 0.75 (green); (**e**) 2D plot of β-derivative at different values of σ = 0.5 (red), 1 (purple), 0.3 (green); (**f**) 2D plot of CD at different values of σ = 0.5 (red), 1 (purple), 0.3 (green); (**g**) A comparison between M-TD (red), β-derivative (blue) and CD (green) at $\sigma = 0.5$. (**d**–**g**) 2D comparison plots at $t = 1$.

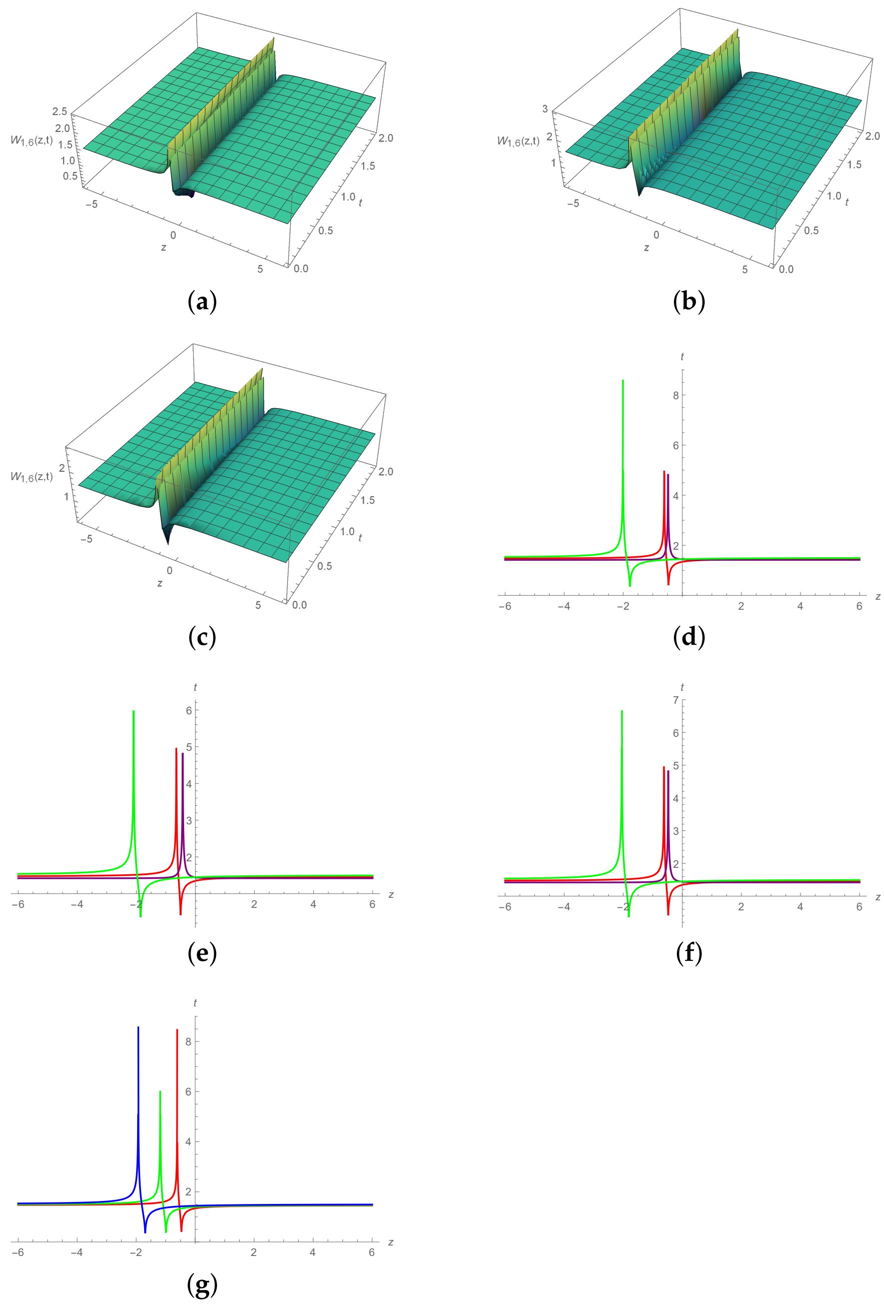

Figure 5. Graphical representation of analytical solution $W_{1,6}(z,t)$ by RB sub-ODE method, when $\sigma = 0.5$, $P = 5.5$, $K = 10.5$, $R = 0.5$, $\beta = 0.35$. (**a**) M-TD 3D graph at σ = 0.5; (**b**) β-derivative 3D graph at σ = 0.5; (**c**) CD 3D graph at σ = 0.5; (**d**) 2D plot of M-TD at different values of σ = 0.5, β = 0.25 (red), σ = 1, β = 0.5 (purple), σ = 0.3, β = 0.75 (green); (**e**) 2D plot of β-derivative at different values of σ = 0.5 (red), 1 (purple), 0.3 (green); (**f**) 2D plot of CD at different values of σ = 0.5 (red), 1 (purple), 0.3 (green); (**g**) A comparison between M-TD (red), β-derivative (blue) and CD (green) at $\sigma = 0.5$. (**d**–**g**) 2D comparison plots at $t = 1$.

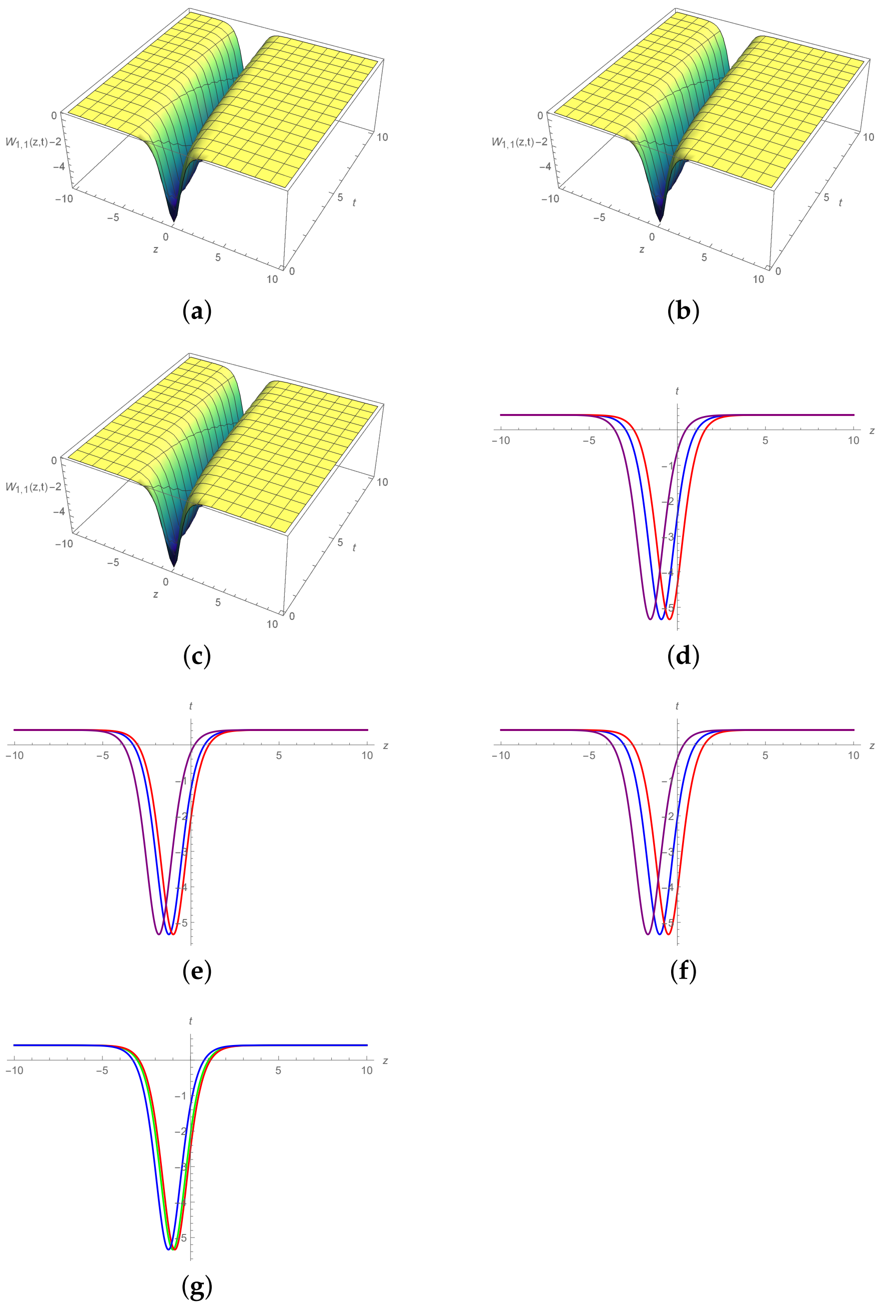

Figure 6. Graphical representation of analytical solution $W_{1,1}(z,t)$ by MAEM, when $K = 2$, $m = 0.1, s = 1, n = 0.1, R = 1, \sigma = 0.5, \beta = 0.35$. (**a**) M-TD 3D graph at σ = 0.5; (**b**) β-derivative 3D graph at σ = 0.5; (**c**) CD 3D graph at σ = 0.5; (**d**) 2D plot of M-TD at different values of σ = 0.5, β = 0.25 (blue), σ = 1, β = 0.5 (red), σ = 0.3, β = 0.75 (purple); (**e**) 2D plot of β-derivative at different values of σ = 0.5 (blue), 1 (red), 0.3 (purple); (**f**) 2D plot of CD at different values of σ = 0.5 (blue), 1 (red), 0.3 (purple); (**g**) A comparison between M-TD (red), β-derivative (blue) and CD (green) at $\sigma = 0.5$. (**d**–**g**) 2D comparison plots at $t = 1$.

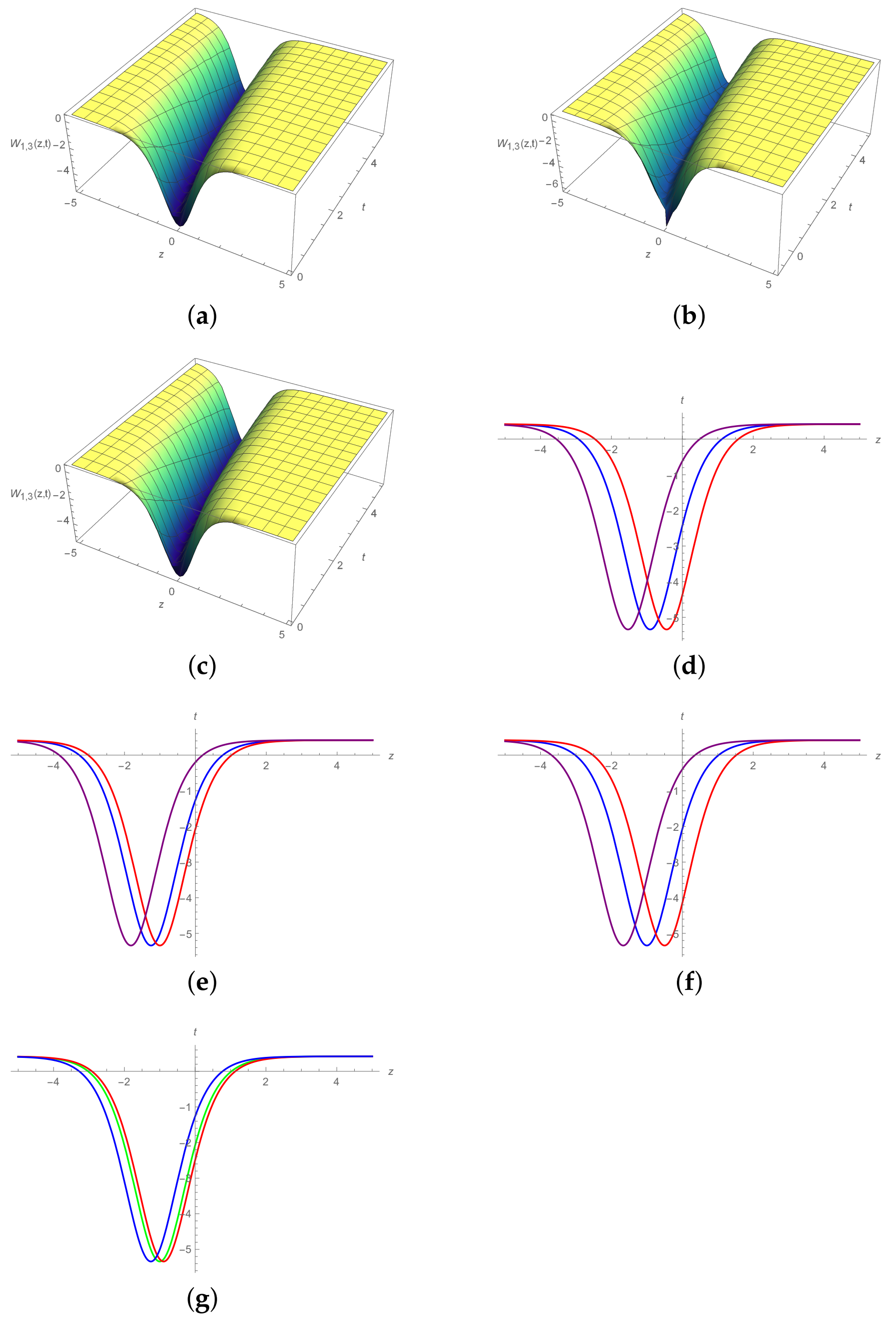

Figure 7. Graphical representation of analytical solution $W_{1,3}(z,t)$ by MAEM, when $K = 2$, $m = 0.1, s = 1, n = 0.1, R = 1, \sigma = 0.5, \beta = 0.35$. (**a**) M-TD 3D graph at σ = 0.5; (**b**) β-derivative 3D graph at σ = 0.5; (**c**) CD 3D graph at σ = 0.5; (**d**) 2D plot of M-TD at different values of σ = 0.5, β = 0.25 (blue), σ = 1, β = 0.5 (red), σ = 0.3, β = 0.75 (purple); (**e**) 2D plot of β-derivative at different values of σ = 0.5 (blue),1 (red), 0.3 (purple); (**f**) 2D plot of CD at different values of σ = 0.5 (blue), 1 (red), 0.3 (purple); (**g**) A comparison between M-TD(red), β-derivative (blue) and CD (green) at $\sigma = 0.5$. (**d**–**g**) 2D comparison plots at $t = 1$.

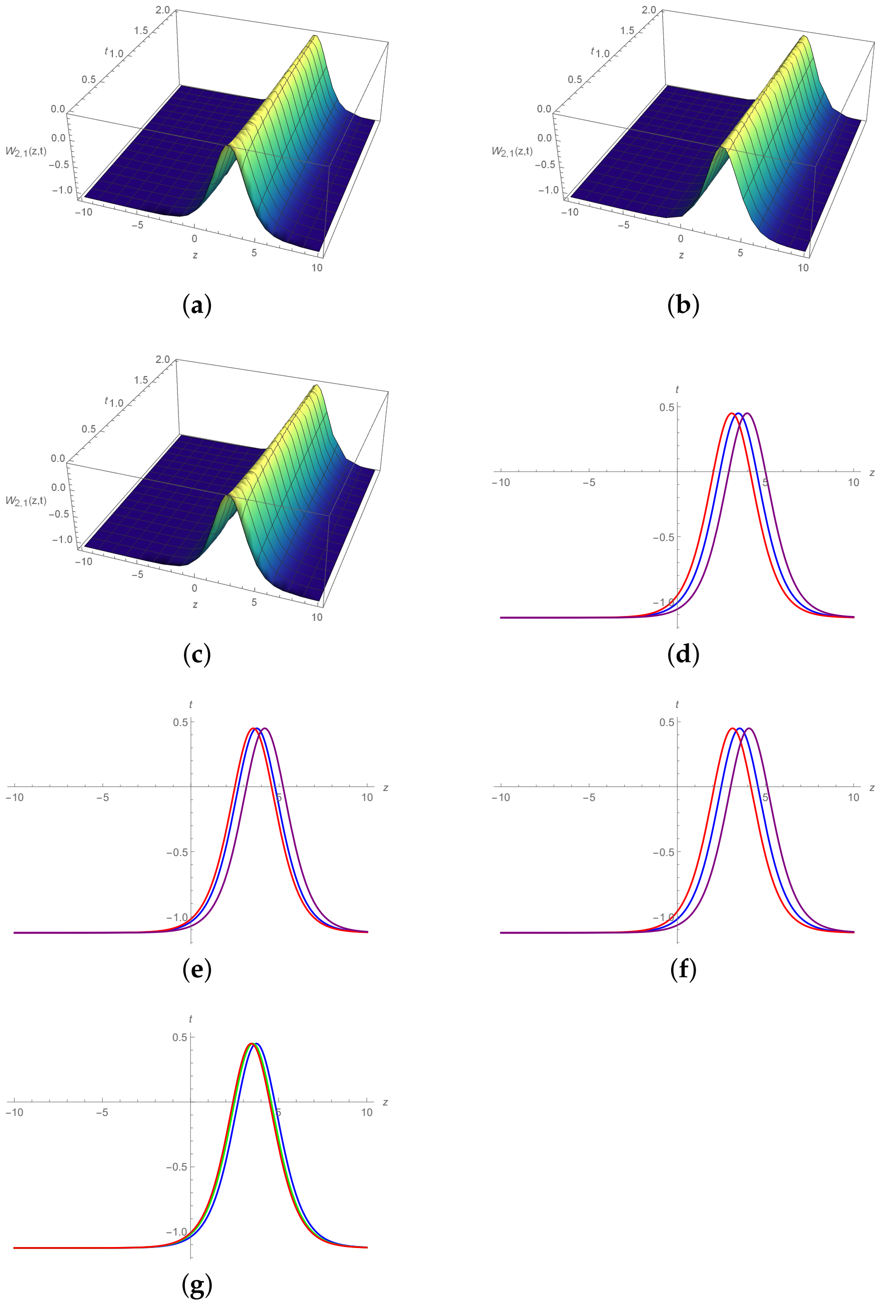

Figure 8. Graphical representation of analytical solution $W_{2,1}(z,t)$ by MAEM, when $K = -2.5$, $m = 0.1, s = 0.5, n = 0.1, R = 1, \sigma = 0.5, \beta = 0.35$. (**a**) M-TD 3D graph at σ = 0.5; (**b**) β-derivative 3D graph at σ = 0.5; (**c**) CD 3D graph at σ = 0.5; (**d**) 2D plot of M-TD at different values of σ = 0.5, β = 0.25 (blue), σ =1, β = 0.5 (red) , σ = 0.3, β = 0.75 (purple); (**e**) 2D plot of β-derivative at different values of σ = 0.5 (blue),1 (red), 0.3 (purple); (**f**) 2D plot of CD at different values of σ = 0.5 (blue), 1 (red), 0.3 (purple); (**g**) A comparison between M-TD (red), β-derivative (blue) and CD (green) at $\sigma = 0.5$. (**d**–**g**) 2D comparison plots at $t = 1$.

In Figures 10 and 11, the trigonometric and hyperbolic solutions of $W_{3,1}(z,t)$ and $W_{3,3}(z,t)$, we receive the M-shape and W-shape soliton solutions, respectively, by choosing the values $\sigma = 0.5$, $\mathrm{m} = 1$, $\mathrm{K} = -1$, $\mathrm{R} = 0.5$, $\beta = 0.35$, $\mathrm{s} = 0.1$, $\mathrm{n} = 1$, within the domain $-10 \leq y \leq 10, 0 \leq t \leq 5$, and $\mathrm{t} = 1$ for 2D surfaces by MAEM. In applied sciences, particularly in dispersive systems, the retrieved solutions are important for describing a variety of natural phenomena.

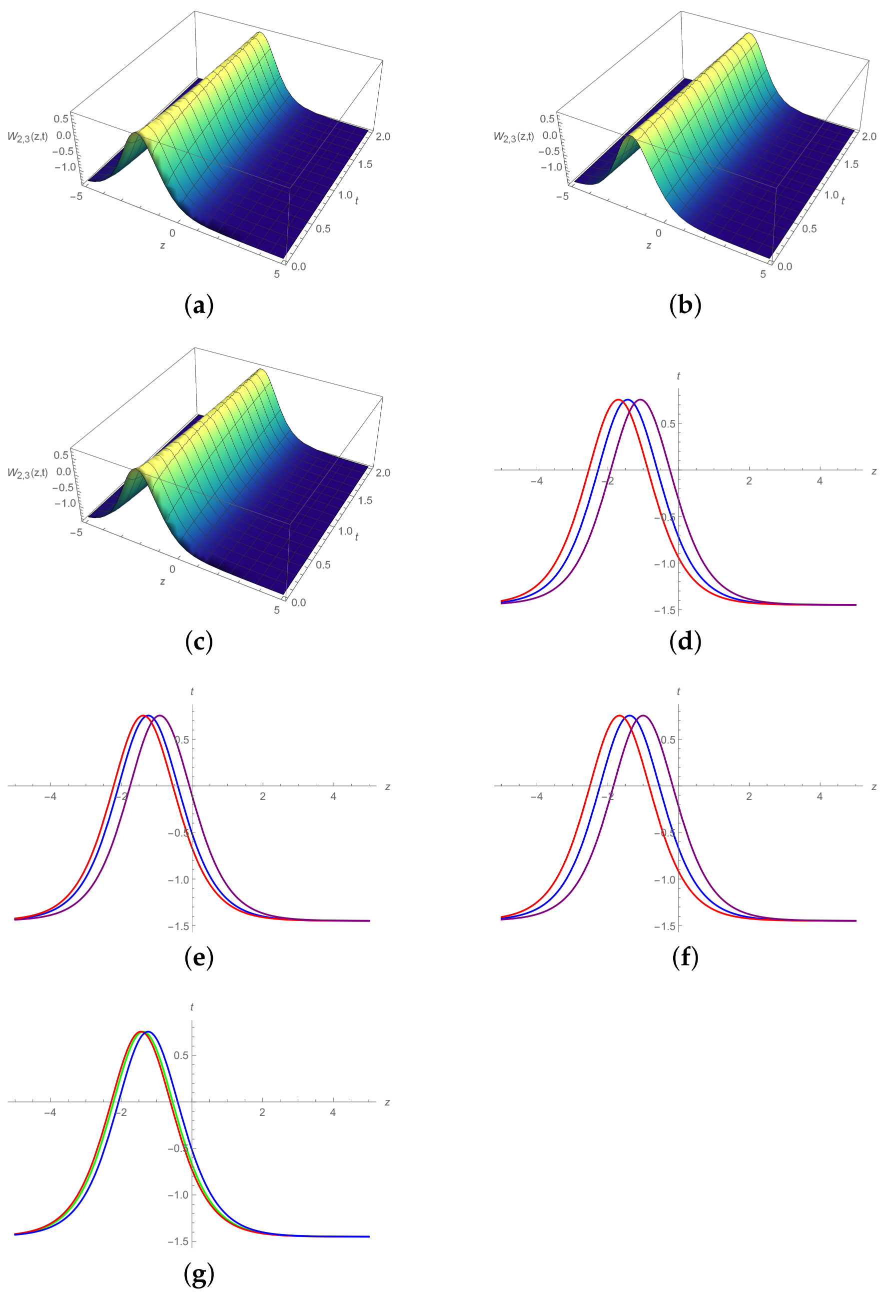

Figure 9. Graphical representation of analytical solution $W_{2,3}(z,t)$ by MAEM, when $K = 3.5$, $m = 0.1, s = 0.5, n = 0.1, R = -1, \sigma = 0.5, \beta = 0.35$. (**a**) M-TD 3D graph at σ = 0.5; (**b**) β-derivative 3D graph at σ = 0.5; (**c**) CD 3D graph at σ = 0.5; (**d**) 2D plot of M-TD at different values of σ = 0.5, β = 0.25 (blue), σ =1, β = 0.5 (red) , σ = 0.3, β = 0.75(purple); (**e**) 2D plot of β-derivative at different values of σ = 0.5 (blue),1 (red), 0.3 (purple); (**f**) 2D plot of CD at different values of σ = 0.5 (blue), 1 (red), 0.3 (purple); (**g**) A comparison between M-TD (red), β-derivative (blue) and CD (green) at $\sigma = 0.5$. (**d**–**g**) 2D comparison plots at $t = 1$.

The construction of dark and bright solitons can be seen in Figure 1. The RB sub-ODE technique provides solutions in the algebraic form in Figure 1, the periodic form in Figure 2, and the hyperbolic form in Figure 3. The MAEM also gives trigonometric in Figures 6, 8 and 10 and hyperbolic in Figures 7, 9 and 11 solutions. The bell-shaped soliton in Figure 9, W-shaped soliton in Figure 10 and M-shaped soliton in Figure 11 are also achieved in this work. These graphs demonstrate the dynamical and dispersive behavior of the solitary wave solutions with a suitable choice of parameters. It can be noticed that the wave profile slightly varies when the fractional parameter's value is changed without changing the form of the curve. A very useful comparison among the different fractional derivatives, including β, conformable, and M-TD's, is shown in two-dimensional line graphs.

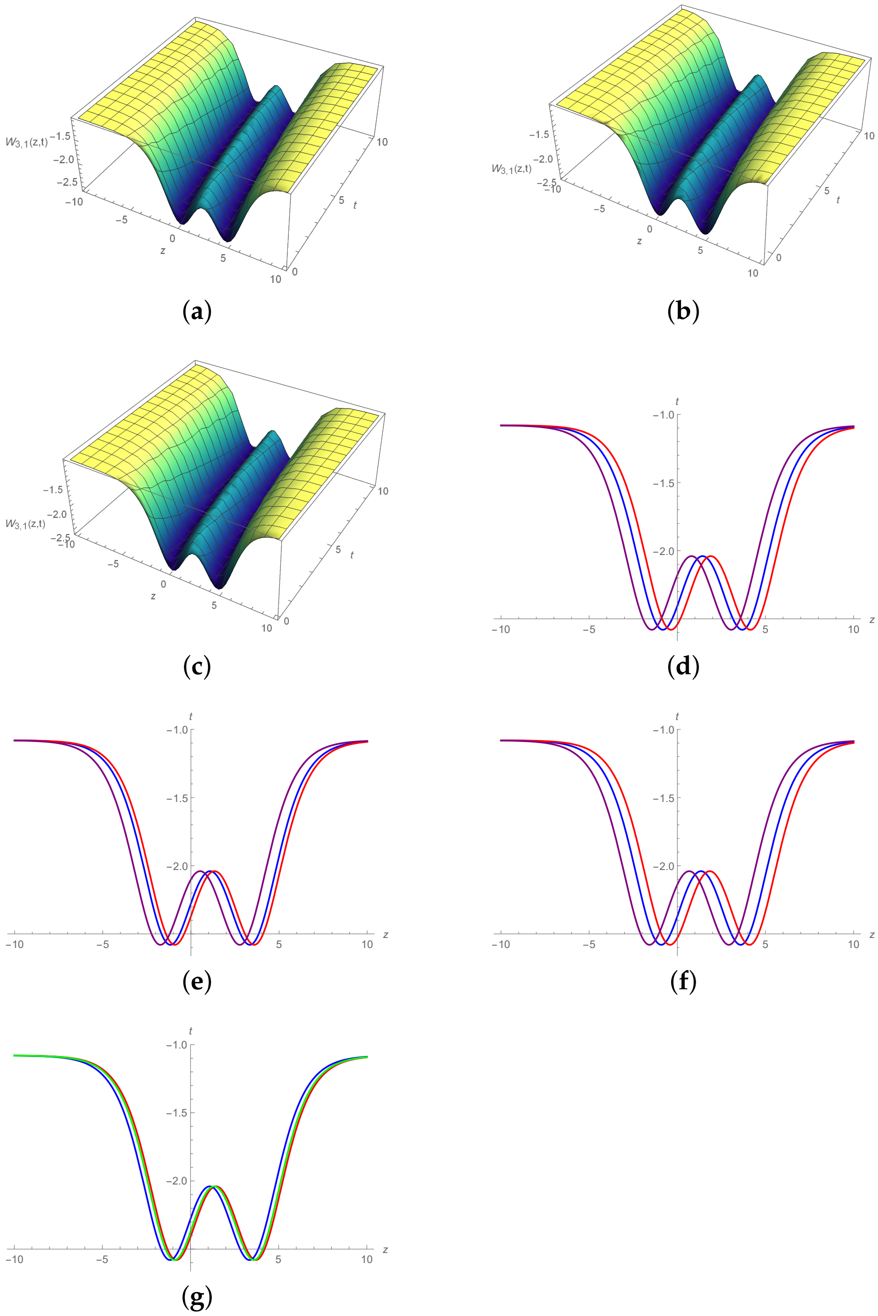

Figure 10. Graphical representation of analytical solution $W_{3,1}(z,t)$ by MAEM, when $K = -1$, $m = 0.1, s = 1, n = 0.1, R = -0.5, \sigma = 0.5, \beta = 0.35$. (**a**) M-TD 3D graph at σ = 0.5; (**b**) β-derivative 3D graph at σ = 0.5; (**c**) CD 3D graph at σ = 0.5; (**d**) 2D plot of M-TD at different values of σ = 0.5, β = 0.25 (blue), σ =1, β = 0.5 (red) , σ = 0.3, β = 0.75 (purple); (**e**) 2D plot of β-derivative at different values of σ = 0.5 (blue),1 (red), 0.3 (purple); (**f**) 2D plot of CD at different values of σ = 0.5 (blue), 1 (red), 0.3 (purple); (**g**) A comparison between M-TD (red), β-derivative (blue) and CD (green) at $\sigma = 0.5$. (**d**–**g**) 2D comparison plots at $t = 1$.

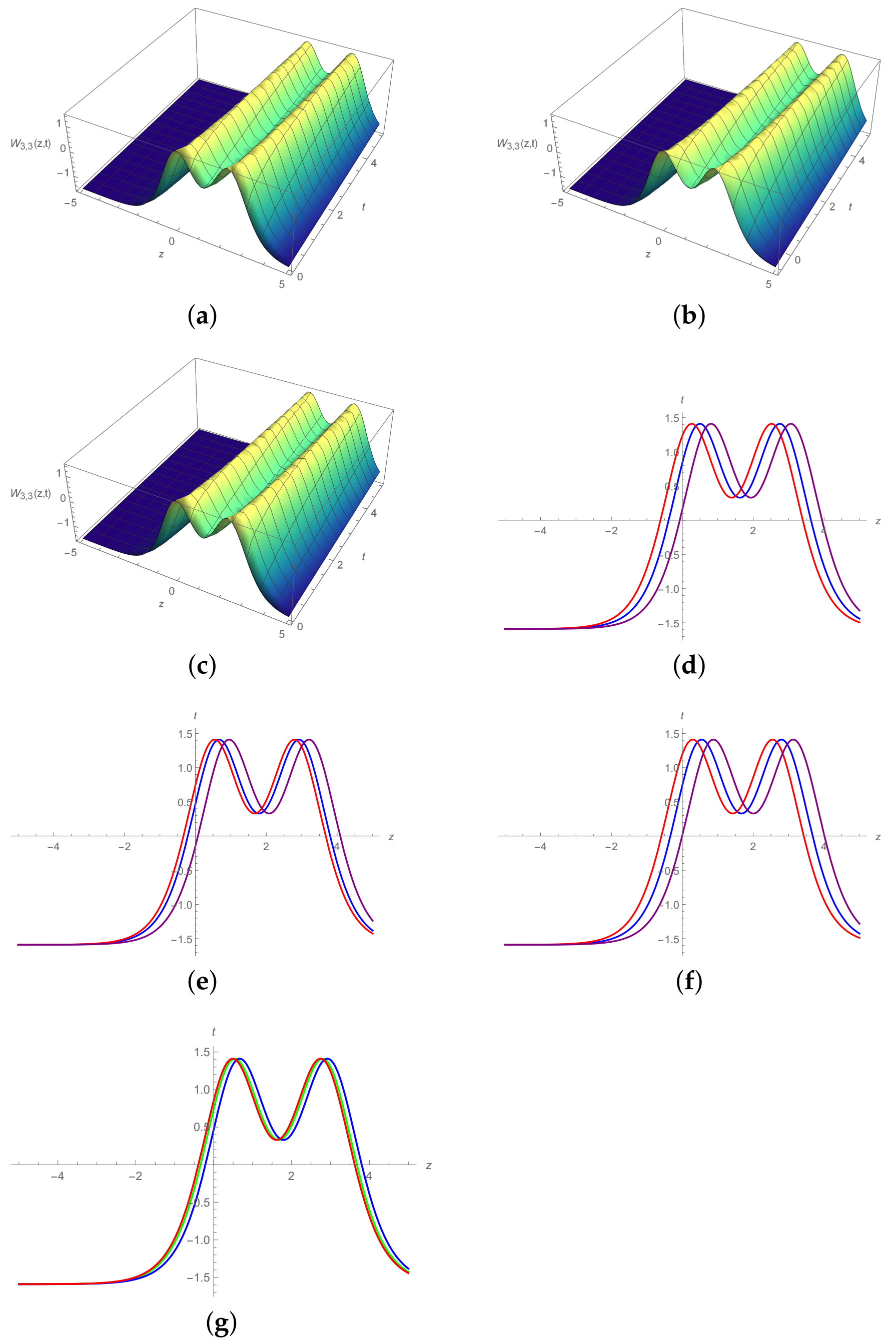

Figure 11. Graphical representation of analytical solution $W_{3,3}(z,t)$ by MAEM, when $K = -2$, $m = 0.1, s = 1, n = 0.1, R = 0.5, \sigma = 0.5, \beta = 0.35$. (**a**) M-TD 3D graph at σ = 0.5; (**b**) β-derivative 3D graph at σ = 0.5; (**c**) CD 3D graph at σ = 0.5; (**d**) 2D plot of M-TD at different values of σ = 0.5, β = 0.25 (blue), σ =1, β = 0.5 (red) , σ = 0.3, β = 0.75 (purple); (**e**) 2D plot of β-derivative at different values of σ = 0.5 (blue),1 (red), 0.3 (purple); (**f**) 2D plot of CD at different values of σ = 0.5 (blue), 1 (red), 0.3 (purple); (**g**) A comparison between M-TD (red), β-derivative (blue) and CD (green) at $\sigma = 0.5$. (**d**–**g**) 2D comparison plots at $t = 1$.

7. Conclusions

In this study, the RB sub-ODE approach and the MAEM were used to solve the nonlinear BBM-Burger problem, yielding novel, accurate, and analytical solitary wave solutions. These methods provided remarkable solutions that can be operated consistently and simply. Using these conventional and computerized techniques, we could comprehend difficult nonlinear differential equations in a range of scientific domains. The solitons and other traveling wave solutions of the governing model could be found by applying the definitions of derivatives with fractional parameters, i.e., β-derivative, CD, and M-TD, to each function. Trigonometric and hyperbolic function solutions could be found in the extracted solutions. The outcomes indicated that the MAEM and RB sub-ODE approaches might be used as helpful mathematical tools for extracting the various solitary wave solutions with different differential operators. The current work can be modified in the future to include more evolution equation kinds with various nonlinearities. This paper has studied the comparison of three derivatives. The analysis says that by changing the values of fractional parameters, an effect on wave solutions is observed but M-TD is considered more valuable because, by changing its parameter values, a smooth wave has been observed. This transitive is very effective and useful. The reason for smooth waves is the Mittag–Leffler function of one parameter, which is why better results are obtained in comparison with other derivatives. They can be used by the researcher in the next phases as well. Future research on the BBM-Burger equation may explore the fractional impacts on the solutions of the governing system using, the fractional local derivative, the Atangana–Baleanu derivative, and other recently proposed definitions of fractional derivatives. We can also consider the BBM-Burger equation with stochastic terms. This study confirms that the RB sub-ODE approach and MAEM are effective and useful mathematical methods and are applicable to investigating other fractional NLEEs in science and engineering.

Author Contributions: Conceptualization, R.A. and M.A.; Formal analysis, R.A., M.A. and F.A.A.; Funding acquisition, X.W. and K.M.A.; Investigation, X.W., R.A., M.A., F.A.A. and K.M.A.; Methodology, X.W., R.A., M.A., F.A.A. and K.M.A.; Project administration, X.W., M.A. and K.M.A.; Software, R.A. and M.A.; Supervision, M.A.; Validation, X.W., R.A. and M.A.; Writing—original draft, X.W., R.A., M.A., F.A.A. and K.M.A.; Writing—review & editing, X.W., R.A., M.A. and K.M.A. All authors have read and agreed to the published version of the manuscript.

Funding: This research received no external funding.

Institutional Review Board Statement: Not applicable.

Informed Consent Statement: Not applicable.

Data Availability Statement: Not applicable.

Acknowledgments: The research of X. Wang is supported by the Science and Technology Foundation of Jiangxi Provincial Department of Education (Grant No. GJJ2201802) and the National Natural Science Foundation of China (Grant No. 11861053). The researchers would like to acknowledge Deanship of Scientific Research, Taif university for funding this work.

Conflicts of Interest: The authors declare no conflict of interest.

Abbreviations

The following abbreviations are used in this manuscript:

BBM-Burger	Benjamin–Bona–Mahony–Burger
MAEM	Modified auxiliary equation method
RB	Ricatti–Bernoulli
CD	Conformable derivative
M-TD	M-truncated derivatives
DEs	Differential equations
NLPDEs	Nonlinear partial differential equations
FDEs	Fractional differential equations
FC	Fractional calculus
FDs	Fractional derivatives
β-derivative	Beta-derivative
JEFM	Jacobi elliptic function method

References

1. Ablowitz, M.J.; Ramani, A.; Segur, H. Nonlinear evolution equations and ordinary differential equations of Painleve'type. *Lett. Nuovo Cim.* **1978**, *23*, 333–338. [CrossRef]
2. Renardy, M.; Rogers, R.C. *An Introduction to Partial Differential Equations*; Springer Science & Business Media: Berlin/Heidelberg, Germany, 2006; Volume 13.
3. Podlubny, I. *Fractional Differential Equations: An Introduction to Fractional Derivatives, Fractional Differential Equations, to Methods of Their Solution and Some of Their Applications*; Academic Press: New York, NY, USA, 1998; p. 198.
4. Oldham, K.B.; Spanier, J. *The Fractional Calculus*; Academic Press: New York, NY, USA, 1974.
5. Singh, J.; Kumar, D.; Al Qurashi, M.; Baleanu, D. A new fractional model for giving up smoking dynamics. *Adv. Differ. Equ.* **2017**, *2017*, 88. [CrossRef]
6. Caputo, M.; Mainardi, F. A new dissipation model based on memory mechanism. *Pure Appl. Geophys.* **1971**, *91*, 134–147. [CrossRef]
7. Caputo, M.; Fabricio, M. A new definition of fractional derivative without singular kernel. *Prog. Fract. Differ. Appl.* **2019**, *1*, 73–85.
8. Atangana, A.; Baleanu, D. New fractional derivatives with nonlocal and non-singular kernel. Theory and application to heat transfer model. *Therm. Sci.* **2016**, *20*, 763–769. [CrossRef]
9. Khalil, R.; Al Horani, M.; Yousef, A.; Sababheh, M. A new definition of fractional derivative. *J. Comput. Appl. Math.* **2014**, *264*, 65–70. [CrossRef]
10. Almeida, R. Caputo–Hadamard fractional derivatives of variable order. *Numer. Funct. Anal. Optim.* **2017**, *38*, 1–19. [CrossRef]
11. Anderson, D.R.; Ulness, D.J. Properties of the Katugampola fractional derivative with potential application in quantum mechanics. *J. Math. Phys.* **2015**, *56*, 063502. [CrossRef]
12. Amado Mendez Cruz, G.; Torres Ledesma, C.E. Multiplicity of solutions for fractional Hamiltonian systems with Liouville-Weyl fractional derivatives. *Fract. Calc. Appl. Anal.* **2015**, *18*, 875–890. [CrossRef]
13. Jumarie, G. Modified Riemann-Liouville derivative and fractional Taylor series of nondifferentiable functions further results. *Comput. Math. Appl.* **2006**, *51*, 1367–1376. [CrossRef]
14. Hanna, L.M.; Luchko, Y.F. Operational calculus for the Caputo-type fractional Erdélyi–Kober derivative and its applications. *Integral Transform. Spec. Funct.* **2014**, *25*, 359–373. [CrossRef]
15. Huang, F.; Liu, F. The space-time fractional diffusion equation with Caputo derivatives. *J. Appl. Math. Comput.* **2005**, *19*, 179–190. [CrossRef]
16. Kumar, V.; Gupta, R.K.; Jiwari, R. Painlevé analysis, Lie symmetries and exact solutions for variable coefficients Benjamin-Bona-Mahony-Burger (BBMB) equation. *Commun. Theor. Phys.* **2013**, *60*, 175. [CrossRef]
17. Hirota, R. Exact solution of the Korteweg—de Vries equation for multiple collisions of solitons. *Phys. Rev. Lett.* **1971**, *27*, 1192. [CrossRef]
18. Jena, S.R.; Senapati, A. On numerical soliton and convergence analysis of Benjamin-Bona-Mahony-Burger equation via octic B-spline collocation. *Arab. J. Basic Appl. Sci.* **2023**, *30*, 146–163. [CrossRef]
19. Alharbi, F.M.; Baleanu, D.; Ebaid, A. Physical properties of the projectile motion using the conformable derivative. *Chin. J. Phys.* **2019**, *58*, 18–28. [CrossRef]
20. Wang, X.; Ehsan, H.; Abbas, M.; Akram, G.; Sadaf, M.; Abdeljawad, T. Analytical solitary wave solutions of a time-fractional thin-film ferroelectric material equation involving beta-derivative using modified auxiliary equation method. *Results Phys.* **2023**, *48*, 106411. [CrossRef]
21. Mohammed, W.W.; Al-Askar, F.M.; Cesarano, C.; Aly, E.S. The Soliton Solutions of the Stochastic Shallow Water Wave Equations in the Sense of Beta-Derivative. *Mathematics* **2023**, *11*, 1338. [CrossRef]
22. Martínez, F.; Martínez, I.; Kaabar, M.K.; Paredes, S. Generalized conformable mean value theorems with applications to multivariable calculus. *J. Math.* **2021**, *2021*, 5528537. [CrossRef]
23. Hussain, A.; Jhangeer, A.; Abbas, N.; Khan, I.; Sherif, E.S.M. Optical solitons of fractional complex Ginzburg-Landau equation with conformable, beta, and M-truncated derivatives: A comparative study. *Adv. Differ. Equ.* **2020**, *2020*, 612. [CrossRef]
24. Mohammed, W.W.; Cesarano, C.; Al-Askar, F.M. Solutions to the (4+1)-Dimensional Time-Fractional Fokas Equation with M-Truncated Derivative. *Mathematics* **2022**, *11*, 194. [CrossRef]
25. Akram, G.; Gillani, S.R. Sub pico-second Soliton with Triki–Biswas equation by the extended $(\frac{G'}{G^2})$-expansion method and the modified auxiliary equation method. *Optik* **2021**, *229*, 166227. [CrossRef]
26. Wan, P.; Manafian, J.; Ismael, H.F.; Mohammed, S.A. Investigating one-, two-, and triple-wave solutions via multiple exp-function method arising in engineering sciences. *Adv. Math. Phys.* **2020**, *2020*, 8018064. [CrossRef]
27. He, X.J.; Lü, X. M-lump solution, soliton solution and rational solution to a (3+1)-dimensional nonlinear model. *Math. Comput. Simul.* **2022**, *197*, 327–340. [CrossRef]
28. Rehman, H.U.; Iqbal, I.; Subhi Aiadi, S.; Mlaiki, N.; Saleem, M.S. Soliton solutions of Klein–Fock–Gordon equation using Sardar subequation method. *Mathematics* **2022**, *10*, 3377. [CrossRef]
29. Parkes, E.J.; Duffy, B.R.; Abbott, P.C. The Jacobi elliptic-function method for finding periodic-wave solutions to nonlinear evolution equations. *Phys. Lett. A* **2002**, *295*, 280–286. [CrossRef]
30. Yusuf, A.; Inc, M.; Aliyu, A.I.; Baleanu, D. Optical solitons possessing beta derivative of the Chen-Lee-Liu equation in optical fibers. *Front. Phys.* **2019**, *7*, 34. [CrossRef]

31. Hassan, S.Z.; Abdelrahman, M.A. A Riccati–Bernoulli sub-ODE method for some nonlinear evolution equations. *Int. J. Nonlinear Sci. Numer. Simul.* **2019**, *20*, 303–313. [CrossRef]
32. Arife, A.S. The modified variational iteration transform method (MVITM) for solve non linear partial differential equation (NLPDE). *World Appl. Sci. J.* **2011**, *12*, 2274–2278. [CrossRef]
33. Jiong, S. Auxiliary equation method for solving nonlinear partial differential equations. *Phys. Lett. A* **2003**, *309*, 387–396. [CrossRef]
34. Akram, G.; Sadaf, M.; Abbas, M.; Zainab, I.; Gillani, S.R. Efficient techniques for traveling wave solutions of time-fractional Zakharov–Kuznetsov equation. *Math. Comput. Simul.* **2022**, *193*, 607–622. [CrossRef]
35. Al-Askar, F.M.; Cesarano, C.; Mohammed, W.W. Abundant Solitary Wave Solutions for the Boiti–Leon–Manna–Pempinelli Equation with M-Truncated Derivative. *Axioms* **2023**, *12*, 466. [CrossRef]
36. Al-Askar, F.M.; Cesarano, C.; Mohammed, W.W. The Influence of White Noise and the Beta Derivative on the Solutions of the BBM Equation. *Axioms* **2023**, *12*, 447. [CrossRef]
37. Ghanbari, B.; Baleanu, D. New optical solutions of the fractional Gerdjikov-Ivanov equation with conformable derivative. *Front. Phys.* **2020**, *8*, 167. [CrossRef]
38. Mohammed, W.W.; Al-Askar, F.M.; Cesarano, C.; El-Morshedy, M. Solitary Wave Solutions of the Fractional-Stochastic Quantum Zakharov–Kuznetsov Equation Arises in Quantum Magneto Plasma. *Mathematics* **2023**, *11*, 488. [CrossRef]
39. Sousa, J.V.D.C.; de Oliveira, E.C. A new truncated M-fractional derivative type unifying some fractional derivative types with classical properties. *Int. J. Anal. Appl.* **2018**, *16*, 83–96. [CrossRef]
40. Ozdemir, N.; Esen, H.; Secer, A.; Bayram, M.; Yusuf, A.; Sulaiman, T.A. Optical solitons and other solutions to the Hirota–Maccari system with conformable, M-truncated and beta derivatives. *Mod. Phys. Lett. B* **2022**, *36*, 2150625. [CrossRef]